

Reflection at the free surface of magneto-thermo-microstretch elastic solid

R. KUMAR* and RUPENDER

Department of Mathematics, Kurukshetra University, Kurukshetra-136 119, India

Abstract. The present investigation is concerned with the reflection in thermo-microstretch elastic solid in the presence of a transverse magnetic field, at the boundary surface. The generalized theories of thermoelasticity developed by Lord and Shulman [1](L-S) and Green and Lindsay [2](G-L) theories have been used to investigate the problem. The variations of amplitude ratios with angle of incidence have been shown graphically. It is noticed that the amplitude ratios of the reflected waves are affected by magnetic field, stretch and thermal properties of the medium.

Key words: magneto-thermo-microstretch elastic solid, amplitude ratios.

1. Introduction

The theory of thermoelasticity deals with the effect of mechanical and thermal disturbances on an elastic body. The theory of uncoupled thermoelasticity consists of the heat equation, which is independent of mechanical effects, and the equation of motion, which contains the temperature as a known function. There are two defects in this theory. First is that the mechanical state of the body has no effect on the temperature. Second, the heat equation, which is parabolic, implies that the speed of propagation of the temperature is infinite, which contradicts physical experiments.

Biot [3] introduced the theory of coupled thermoelasticity to overcome the first shortcoming. The governing equations for this theory are coupled, eliminating the first paradox of the classical theory. However, both theories share the second shortcoming since the heat equation for the coupled theory is also parabolic. To overcome this drawback, two generalizations to the coupled theory were introduced.

The first is due to Lord and Shulman [1], who obtained a wave-type heat equation by postulating a new law of heat conduction to replace the classical Fourier's law. This new law contains the heat flux vector as well as its time derivative. It contains also a new constant that act as a relaxation time. Since the heat equation of this theory is of the wave-type, it automatically ensures finite speeds of propagation for heat and elastic waves. The remaining governing equations for this theory, namely, the equations of motion and constitutive relations, remain the same as those for the coupled and uncoupled theories.

The second generalization to the coupled theory of elasticity is what is known as the theory of thermoelasticity with two relaxation times or the theory of temperature-rate-dependent thermoelasticity. Mullar [4], in a review of the thermodynamics of thermoelastic solids, proposed an entropy production inequality, with the help of which he considered restrictions

on a class of constitutive equations. A generalization of this inequality was proposed by Green and Laws [5]. Green and Lindsay obtained another version of the constitutive equations in [2]. These equations were also obtained independently and more explicitly by Suhubi [6]. This theory contains two constants that act as relaxation times and modify all the equations of the coupled theory, not only the heat equation. The classical Fourier's law of heat conduction is not violated if the medium under consideration has a center of symmetry.

Eringen [7] developed the theory of micropolar elastic solids with stretch by include the effect of axial stretch during the rotation of molecules. The mechanical model underlying this theory can be envisioned as an elastic medium composed of a large number of short springs. These springs possess average inertia moments and can deform in axial directions. The material points in this continuum possess not only classical translational degree of freedom represented by the deformation vector field but also intrinsic rotations and an intrinsic axial stretch. The difference between these solids and micropolar elastic solids stems from the presence of a scalar microstretch and a vector first moment. These solids can undergo intrinsic volume change independent of the macro-volume change. This is accompanied by a non-deviatoric stress moment vector.

Eringen [8] developed a theory of thermo-microstretch elastic solid in which he included microstructural expansions and contractions. Eringen [9] also derived the equations of motions, constitutive equations and boundary conditions for thermo-microstretch fluids and obtain the solution of the problem for acoustical waves in bubbly liquids. Microstretch continuum is a model for Bravias lattice with a basis on the atomic level and a two phase dipolar solid with a core on the macroscopic level. The material points of microstretch bodies can stretch and contract independently of their translations and rotations. For example, composite materials reinforced with

*e-mail: rajneesh_kuk@rediffmail.com

chopped elastic fibers, porous media whose pores are filled with gas or inviscid liquid, asphalt or other elastic inclusions and 'solid-liquid' crystals, etc. should be characterizable by microstretch solids.

The linear theory of micropolar thermoelasticity was developed by extending the theory of micropolar continua to include thermal effects by Eringen [10] and Nowacki [11]. Chandrasekhariah [12] formulated a theory of micropolar thermoelasticity which includes heat flux, among the constitutive variables.

Kalaski and Nowacki [13] investigated the wave type of equations of thermo-magneto-microelasticity. Nowacki [14] studied some problems of micropolar magnetoelasticity.

Kumar and Singh [15, 16] discussed the problems of wave propagation in a micropolar generalized thermoelastic body with stretch and in a generalized thermo-microstretch elastic solid. Kumar and Singh [17] studied the reflection of plane waves from the flat boundary of a micropolar generalized thermoelastic half space with stretch. Tomar and Garg [18] discussed reflection and transmission of waves from a plane interface between two microstretch solid half-space. Kumar and Pratap [19] studied reflection of plane waves in a heat flux dependent microstretch thermoelastic solid half space. Kumar, Pathania and Sharma [20] investigated the propagation of Rayleigh-Lamb waves in thermo-microstretch elastic plates. In spite of these studies, magnetic effect on the propagation of waves in generalized thermo-microstretch elastic solid has not been studied.

In this paper, we study the problem of reflection of plane waves at the free surface of the generalized thermo-microstretch elastic solid permeated by transverse magnetic field. Magnetic effect on the amplitude ratios of various reflected waves for the generalized theories of thermoelasticity, with the angle of incidence are computed numerically and presented graphically, for a specific model.

2. Basic equations

The simplified linear equations of electrodynamics of slowly moving medium for a homogenous and perfectly conducting elastic solid are the following:

$$\begin{cases} \epsilon_{ijk} h_{k,j} - (J_i + \epsilon_0 \dot{E}_i) = 0, & \epsilon_{ijk} E_{j,i} + \mu_0 \dot{h}_k = 0, \\ E_i + \mu_0 (\epsilon_{ijk} \dot{u}_j H_{0k}) = 0, & h_{i,i} = 0, \end{cases} \quad (1)$$

Maxwell stress components are given by

$$T_{ij} = \mu_0 (H_i h_j + H_j h_i - H_k h_k \delta_{ij}), \quad (2)$$

where H_{0i} – the external applied magnetic field intensity vector, h_i – the induced magnetic field vector, E_i – the induced electric field vector, J_i – the current density vector, u_i – the displacement vector, μ_0 and ϵ_0 – the magnetic and electric permeabilities respectively, T_{ij} – the components of Maxwell stress tensor and δ_{ij} – the Kroneker delta.

The above Eq. (1) are supplemented by the field of equations of motion and constitutive relations in the theory of generalized thermo-microstretch elastic solid, taking into account the Lorentz force are

$$(\lambda + \mu) u_{j,ij} + (\mu + K) u_{i,jj} + K \epsilon_{ijk} \phi_{k,j} - \nu (T_{,i} + \tau_1 \dot{T}_{,i}) + \lambda_0 \phi_{,i}^* + F_i - \rho \ddot{u}_i = 0, \quad (3)$$

$$(\alpha + \beta) \phi_{j,ij} + \gamma \phi_{i,jj} + K \epsilon_{imn} u_{n,m} - 2K \phi_i - \rho j \ddot{\phi}_i = 0, \quad (4)$$

$$\alpha_0 \phi_{,rr}^* + \nu_1 (T + \tau_1 \dot{T}) - \lambda_1 \phi^* - \lambda_0 u_{j,j} - \frac{1}{2} \rho j_0 \ddot{\phi}^* = 0, \quad (5)$$

$$\rho c^* (\dot{T} + \tau_0 \ddot{T}) + \nu_1 T_0 (\dot{\phi}^* + n_0 \tau_0 \ddot{\phi}^*) + \nu T_0 (\dot{u}_{j,j} + n_0 \tau_0 \ddot{u}_{j,j}) - K^* T_{,rr} = 0, \quad (6)$$

$$\sigma_{ij} = \lambda u_{r,r} \delta_{ij} + \mu (u_{i,j} + u_{j,i}) + K (u_{j,i} - \epsilon_{ijr} \phi_r) - \nu (T + \tau_1 \dot{T}) \delta_{ij}, \quad (7)$$

$$m_{ij} = \alpha \phi_{r,r} \delta_{ij} + \beta \phi_{i,j} + \gamma \phi_{j,i} + b_0 \epsilon_{mji} \phi_{,m}^*, \quad (8)$$

$$\lambda_k = \alpha_0 \phi_{,k}^* + b_0 \epsilon_{klm} \phi_{l,m}, \quad (9)$$

where $\lambda, \mu, K, \alpha, \beta, \gamma, \lambda_1, \lambda_0, \alpha_0, b_0$ – the material constants, T – temperature change, T_0 – uniform temperature, K^* – thermal conductivity, c^* – specific heat at constant temperature, $\nu = (3\lambda + 2\mu + K)\alpha_{t_1}$, $\nu_1 = (3\lambda + 2\mu + K)\alpha_{t_2}$, $\alpha_{t_1}, \alpha_{t_2}$ – linear thermal expansions, τ_0 and τ_1 are thermal relaxation times. ρ – the density, j – the microinertia, ϕ_i – the microrotation vector, ϕ^* – the scalar microstretch and σ_{ij} – the components of force stress tensor, m_{ij} – the components of couple stress tensor, λ_k – the microstretch parameter, ϵ_{ijk} – the alternate tensor. Comma notation denotes partial derivatives with respect to spatial co-ordinate and the superposed dots denote the derivatives with respect to time. The Lorentz force is given by

$$F_i = \mu_0 \epsilon_{ijk} J_j H_{0k}. \quad (10)$$

For L-S theory, $\tau_1 = 0, n_0 = 1$; for G-L theory, $\tau_1 > 0, n_0 = 0$. The thermal relaxations τ_0 and τ_1 satisfy the inequality $\tau_1 \geq \tau_0 > 0$ for G-L theory only.

3. Formulation of the problem

We consider a homogenous, isotropic, perfectly conducting thermo-microstretch elastic medium adjoining with free surface, permeated by an initial magnetic field H_{0i} acting along the z-axis. The rectangular Cartesian co-ordinate system (x, y, z) having origin on the surface $y = 0$ with y-axis pointing vertically into the medium is introduced.

For two dimensional problem, we assume the displacement vector u_i and microrotation vector ϕ_i as

$$u_i = (u, v, 0) \quad \text{and} \quad \phi_i = (0, 0, \phi_3). \quad (11)$$

We define the non-dimensional quantities as

$$\begin{aligned} x' &= \frac{\bar{w}}{c_1} x, & y' &= \frac{\bar{w}}{c_1} y, & u' &= \frac{\rho c_1 \bar{w}}{\nu T_0} u, \\ v' &= \frac{\rho c_1 \bar{w}}{\nu T_0} v, & \sigma'_{ij} &= \frac{\sigma_{ij}}{\nu T_0}, & T'_{ij} &= \frac{T_{ij}}{\nu T_0}, \\ h' &= \frac{h}{H_0}, & m'_{ij} &= \frac{\bar{w}}{c_1 \nu T_0} m_{ij}, & \lambda'_k &= \frac{c_1}{\nu T_0 \bar{w}} \lambda_k, \\ t' &= \bar{w} t, & \tau'_1 &= \bar{w} \tau_1, & \tau'_0 &= \bar{w} \tau_0, \end{aligned}$$

$$\begin{aligned}
 E'_1 &= \frac{E_1}{\mu_0 H_0 c_1}, & E'_2 &= \frac{E_2}{\mu_0 H_0 c_1}, \\
 \phi'_3 &= \frac{\rho c_1^2}{\nu T_0} \phi_3, & \phi^{*'} &= \frac{\rho c_1^2}{\nu T_0} \phi^*, \\
 T' &= \frac{T}{T_0},
 \end{aligned}
 \tag{12}$$

where

$$\begin{aligned}
 \bar{\omega} &= \frac{\rho c^* c_1^2}{K^*}, & c_1^2 &= \frac{\lambda + 2\mu + K}{\rho}, & c_2^2 &= \frac{\mu + K}{\rho}, \\
 c^2 &= \frac{1}{\mu_0 \epsilon_0}, & a_0^2 &= \frac{\mu_0 H_0^2}{\rho}.
 \end{aligned}$$

Expressing the displacement components $u(x, y, t)$, $v(x, y, t)$ by the scalar potential functions $\psi_1(x, y, t)$, $\psi_2(x, y, t)$ in dimensionless form

$$u = \frac{\partial \psi_1}{\partial x} + \frac{\partial \psi_2}{\partial y}, \quad v = \frac{\partial \psi_1}{\partial y} - \frac{\partial \psi_2}{\partial x}
 \tag{13}$$

and using the Eqs. (1), (3)–(6), and (10)–(13), we obtain two coupled system of equations

$$\begin{bmatrix}
 \delta_1^2 \nabla^2 - \delta_2^2 \frac{\partial^2}{\partial t^2} & - \left(1 + \tau_1 \frac{\partial}{\partial t} \right) \\
 -a_1 \left(\frac{\partial}{\partial t} + \tau_0 n_0 \frac{\partial^2}{\partial t^2} \right) \nabla^2 & \nabla^2 - \left(\frac{\partial}{\partial t} + \tau_0 \frac{\partial^2}{\partial t^2} \right) \\
 -a_3 \nabla^2 & a_4 \left(1 + \tau_1 \frac{\partial}{\partial t} \right) \\
 \frac{\lambda_0}{\rho c_1^2} \\
 -a_2 \left(\frac{\partial}{\partial t} + \tau_0 n_0 \frac{\partial^2}{\partial t^2} \right) \\
 \nabla^2 - a_5 \frac{\partial^2}{\partial t^2} - a_6
 \end{bmatrix}
 \begin{bmatrix}
 \psi_1 \\
 T \\
 \phi^*
 \end{bmatrix}
 = \begin{bmatrix}
 0 \\
 0 \\
 0
 \end{bmatrix}
 \tag{14}$$

and

$$\begin{bmatrix}
 \nabla^2 - \frac{c_1^2}{c_2^2} \delta_2^2 \frac{\partial^2}{\partial t^2} & \frac{K}{\rho c_2^2} \\
 -a_7 \nabla^2 & \nabla^2 - a_8 \frac{\partial^2}{\partial t^2} - 2a_7
 \end{bmatrix}
 \begin{bmatrix}
 \psi_2 \\
 \phi_3
 \end{bmatrix}
 = \begin{bmatrix}
 0 \\
 0
 \end{bmatrix}
 \tag{15}$$

where ∇^2 is the Laplacian operator and

$$a_1 = \frac{\nu^2 T_0}{\rho^2 c_1^2 c^*}, \quad a_2 = \frac{\nu \nu_1 T_0}{\rho^2 c_1^2 c^*}, \quad a_3 = \frac{\lambda_0 K^{*2}}{\alpha_0 \rho^2 c^{*2} c_1^2},$$

$$a_4 = \frac{\nu_1 K^{*2}}{\nu \alpha_0 \rho c^{*2}}, \quad a_5 = \frac{\rho J_0 c_1^2}{2 \alpha_0}, \quad a_6 = \frac{\lambda_1 K^{*2}}{\alpha_0 \rho^2 c^{*2} c_1^2},$$

$$a_7 = \frac{K K^*}{\gamma \rho^2 c^{*2} c_1^2}, \quad a_8 = \frac{\rho J}{\gamma c_1^2},$$

$$\delta_1^2 = 1 + \frac{a_0^2}{c_1^2}, \quad \delta_2^2 = 1 + \frac{a_0^2}{c^2},$$

$$\tau_{10} = \tau_1 + i\omega^{-1}, \quad \tau_{20} = \tau_0 + i\omega^{-1}, \quad \tau_{30} = \tau_0 n_0 + i\omega^{-1}.$$

4. Reflection and boundary conditions

We consider a plane wave (thermal(T) wave/longitudinal microstretch(LM) wave/ coupled transverse and microrotational(CD-I) wave) propagating through the generalised magneto-thermo-microstretch elastic solid half space ($y > 0$) and making an angle of incidence θ_0 with the y -axis, at the free surface ($y = 0$). Corresponding to each incident wave, we get reflected longitudinal displacement(LD)wave, thermal(T) wave, longitudinal microstretch(LM) wave, coupled transverse and microrotational(CD-I and CD-II) waves as shown in Fig. 1.

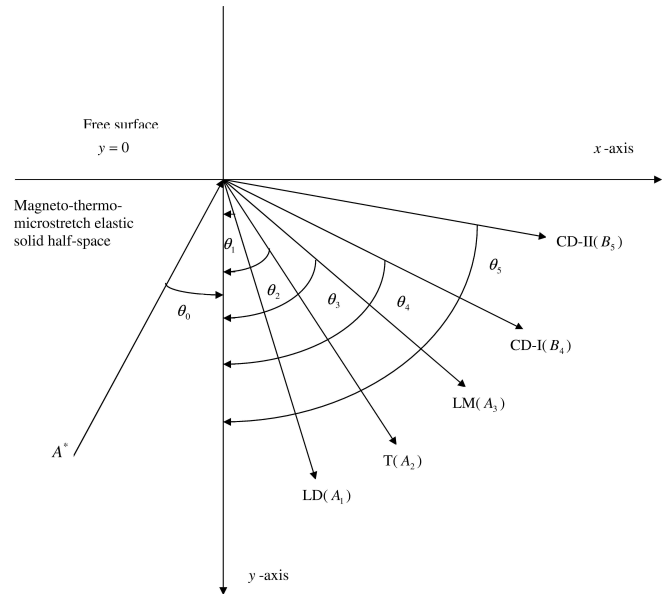


Fig. 1. Geometry of the problem

We assume the solutions of the system of equations (14)–(15) in the form

$$\begin{aligned}
 &\{\psi_1, T, \phi^*, \psi_2, \phi_3\} \\
 &= \{\bar{\psi}_1, \bar{T}, \bar{\phi}^*, \bar{\psi}_2, \bar{\phi}_3\} e^{i\{k(x \sin \theta - y \cos \theta) - \omega t\}},
 \end{aligned}
 \tag{16}$$

where k is the wave number and ω is the complex circular frequency.

Making use of (11)–(13) and (16) in Eq. (14)–(15), we obtain two equations, one is cubic and second is quadratic in V^2 given by

$$V^6 + AV^4 + BV^2 + C = 0,
 \tag{17}$$

$$V^4 + DV^2 + E = 0,
 \tag{18}$$

where $V = \omega/k$ is the velocity of the coupled waves; V_1, V_2, V_3 are the velocities the coupled waves namely longitudinal displacement(LD) wave, thermal(T) wave, longitudinal microstretch(LM) wave respectively given by equation (17) and V_4, V_5 are the velocities of coupled transverse and microrotational (CD-I and CD-II) waves respectively given by equation (18) and

$$\begin{aligned}
 A &= \frac{-1}{\delta_2^2 d_2} \left[\delta_2^2 d_1 + \delta_1^2 d_2 - i\omega\tau_{10}\tau_{30} \right. \\
 &\quad \left. \left\{ a_1 a_5 + \frac{1}{\omega^2} (a_2 a_3 - a_1 a_6) \right\} \right. \\
 &\quad \left. - \frac{\lambda_0}{\rho c_1^2} \left(\frac{i}{\omega} a_1 a_4 \tau_{10} \tau_{30} - \frac{1}{\omega^2} a_3 \right) \right], \\
 B &= \frac{1}{\delta_2^2 d_2} \left[\delta_1^2 d_1 + \delta_2^2 d_2 - i\omega a_1 \tau_{10} \tau_{30} + \frac{\lambda_0}{\rho c_1^2} \left(\frac{1}{\omega^2} a_3 \right) \right], \\
 C &= -\frac{\delta_1^2}{\delta_2^2 d_2}, \\
 D &= \frac{1}{d_3} \left[\frac{1}{\omega^2} \left(2a_7 + \frac{K}{\rho c_2^2} \right) - \left(\frac{c_1^2}{c_2^2} \delta_2^2 + a_8 \right) \right], \\
 E &= \frac{1}{d_3} \\
 d_1 &= a_5 - \frac{a_6}{\omega^2} + \tau_{20}, \\
 d_2 &= a_5 \tau_{20} - \frac{1}{\omega^2} a_6 \tau_{20} + \frac{i}{\omega} a_2 a_4 \tau_{10} \tau_{30}, \\
 d_3 &= \frac{c_1^2}{c_2^2} \delta_2^2 \left(a_8 - 2 \frac{a_7}{\omega^2} \right).
 \end{aligned}$$

Since the boundary $y=0$ is free from surface tractions. The boundary conditions are

$$\begin{aligned}
 \sigma_{22} + T_{22} &= 0, \quad \sigma_{21} = 0, \\
 m_{23} &= 0, \quad \lambda_2 = 0, \quad \frac{\partial T}{\partial y} = 0.
 \end{aligned} \tag{19}$$

In view of equation (16), we assume the values of $\psi_1, T, \phi^*, \psi_2$ and ϕ_3 satisfying the boundary conditions as

$$\{\psi_1, T, \phi^*\} = \sum_{i=1}^3 \{1, \eta_i, \xi_i\} \tag{20}$$

$$[A_{0i} e^{i\{k_i(x \sin \theta_{0i} - y \cos \theta_{0i}) - \omega_i t\}} + P_i],$$

$$\{\psi_2, \phi_3\} = \sum_{j=4}^5 \{1, \eta_j\} \tag{21}$$

$$[B_{0j} e^{i\{k_j(x \sin \theta_{0j} - y \cos \theta_{0j}) - \omega_j t\}} + P_j],$$

where

$$P_i = A_i e^{i\{k_i(x \sin \theta_i + y \cos \theta_i) - \omega_i t\}},$$

$$P_j = B_j e^{i\{k_j(x \sin \theta_j + y \cos \theta_j) - \omega_j t\}},$$

$$\eta_i = \frac{a_1 \omega^2 \tau_{30} \left(-1 + a_5 V_i^2 - a_6 \frac{V_i^2}{\omega^2} \right) + a_2 a_3 V_i^2 \tau_{30}}{(-1 + V_i^2 \tau_{20}) \left(-1 + a_5 V_i^2 - a_6 \frac{V_i^2}{\omega^2} \right) + \frac{i}{\omega} a_2 a_4 V_i^2 \tau_{10} \tau_{30}},$$

$$\xi_i = \frac{i a_1 a_4 \omega V_i^2 \tau_{10} \tau_{30} - a_3 (-1 + V_i^2 \tau_{20})}{(-1 + V_i^2 \tau_{20}) \left(-1 + a_5 V_i^2 - a_6 \frac{V_i^2}{\omega^2} \right) + \frac{i}{\omega} a_2 a_4 V_i^2 \tau_{10} \tau_{30}},$$

$$\eta_j = \frac{-a_7}{-1 + a_8 V_j^2 - 2a_7 \frac{V_j^2}{\omega^2}}, \quad (i = 1, 2, 3 \quad \& \quad j = 4, 5).$$

and A_{0i} are the amplitudes of the incident LD-wave, T-wave, LM-wave, and B_{0j} are the amplitudes of the incident CD-I, CD-II waves respectively. A_i are the amplitudes of the reflected LD-wave, T-wave, LM-wave, and B_j are the amplitudes of the reflected CD-I, CD-II waves respectively (Fig. 1).

In order to satisfy the boundary conditions, the extension of the Snell's law will be

$$\frac{\sin \theta_0}{V_0} = \frac{\sin \theta_1}{V_1} = \frac{\sin \theta_2}{V_2} = \frac{\sin \theta_3}{V_3} = \frac{\sin \theta_4}{V_4} = \frac{\sin \theta_5}{V_5}, \tag{22}$$

where

$$k_1 V_1 = k_2 V_2 = k_3 V_3 = k_4 V_4 = k_5 V_5 = \omega \quad \text{at } y = 0. \tag{23}$$

Making use of potentials given by Eqs. (20)–(21) in boundary conditions (19) and using Eqs. (22) and (23), we get a system of five non-homogeneous equations which can be written as

$$\sum_{i=1}^5 a_{ij} Z_j = Y_i, \quad (j = 1, 2, \dots, 5), \tag{24}$$

where

$$a_{1i} = -r_1 k_i^2 - r_2 k_i^2 \cos^2 \theta_i + i\omega_i \tau_{10} \eta_i + r_3 \xi_i,$$

$$a_{1j} = r_2 k_j^2 \sin \theta_j \cos \theta_j,$$

$$a_{2i} = -(2 + r_4) k_i^2 \sin \theta_i \cos \theta_i,$$

$$a_{2j} = k_j^2 \sin^2 \theta_j - (1 + r_4) k_j^2 \cos^2 \theta_j + r_4 \eta_j,$$

$$a_{3i} = -i r_5 \xi_i k_i \sin \theta_i, \quad a_{3j} = i \eta_j k_j \cos \theta_j,$$

$$a_{4i} = i \xi_i k_i \cos \theta_i, \quad a_{4j} = i r_6 \eta_j k_j \sin \theta_j,$$

$$a_{5i} = i k_i \cos \theta_i, \quad a_{5j} = 0, \quad (i = 1, 2, 3 \quad \& \quad j = 4, 5)$$

and

$$r_1 = \frac{\lambda}{\rho c_1^2} + \delta_1^2 - 1, \quad r_2 = \frac{2\mu + K}{\rho c_1^2}, \quad r_3 = \frac{\lambda_0}{\rho c_1^2},$$

$$r_4 = \frac{K}{\mu}, \quad r_5 = \frac{b_0}{\gamma}, \quad r_6 = \frac{b_0}{\alpha_0},$$

$$Z_1 = \frac{A_1}{A^*}, \quad Z_2 = \frac{A_2}{A^*}, \quad Z_3 = \frac{A_3}{A^*}, \quad Z_4 = \frac{B_4}{A^*}, \quad Z_5 = \frac{B_5}{A^*}. \tag{25}$$

(i) For Incident LD-wave;

$$A^* = A_{01}, \quad A_{02} = A_{03} = B_{04} = B_{05} = 0$$

$$Y_1 = -a_{11}, \quad Y_2 = a_{21}, \quad Y_3 = -a_{31},$$

$$Y_4 = a_{41}, \quad Y_5 = a_{51},$$

(ii) For Incident T-wave;

$$A^* = A_{02}, \quad A_{01} = A_{03} = B_{04} = B_{05} = 0$$

$$Y_1 = -a_{12}, \quad Y_2 = a_{22}, \quad Y_3 = -a_{32},$$

$$Y_4 = a_{42}, \quad Y_5 = a_{52},$$

(iii) For Incident LM-wave;

$$A^* = A_{03}, \quad A_{01} = A_{02} = B_{04} = B_{05} = 0$$

$$Y_1 = -a_{13}, \quad Y_2 = a_{23}, \quad Y_3 = -a_{33},$$

$$Y_4 = a_{43}, \quad Y_5 = a_{53},$$

(iv) For Incident CD(I)-wave;

$$A^*=B_{04}, \quad A_{01} = A_{02} = A_{03} = B_{05} = 0$$

$$Y_1 = a_{14}, \quad Y_2 = -a_{24}, \quad Y_3 = a_{34},$$

$$Y_4 = -a_{44}, \quad Y_5 = 0,$$

(v) For Incident CD(II)-wave;

$$A^*=B_{05}, \quad A_{01} = A_{02} = A_{03} = B_{04} = 0$$

$$Y_1 = a_{15}, \quad Y_2 = -a_{25}, \quad Y_3 = a_{35},$$

$$Y_4 = -a_{45}, \quad Y_5 = 0,$$

and

$$V_0 = \begin{cases} V_1 & \text{for incident LD - wave,} \\ V_2 & \text{for incident T - wave,} \\ V_3 & \text{for incident LM - wave,} \\ V_4 & \text{for incident (CD-I) - wave,} \\ V_5 & \text{for incident (CD-II) - wave} \end{cases} \quad (26)$$

In the absence of magnetic field and stretch effect, our results tally with the results of Singh and Kumar [21], by changing the dimensionless quantities into the physical quantities.

5. Numerical results and discussion

Following Gauthier [22], the values of micropolar constants are

$$\lambda = 7.59 \times 10^9 Nm^{-2}, \quad \mu = 1.89 \times 10^9 Nm^{-2},$$

$$K = .0149 \times 10^9 Nm^{-2}, \quad \rho = 2.638 \times 10^3 Kg m^{-3},$$

$$\gamma = 2.63 \times 10^3 N, \quad j = 0.196 \times 10^{-6} m^2.$$

and other parameters are taken

$$c^* = 0.9614 \times 10^3 Jkg^{-1} Kelvin^{-1},$$

$$K^* = 2.502 Jm^{-1} sec^{-1} Kelvin^{-1},$$

$$\alpha_{t1} = 0.5 \times 10^{-3} Kelvin^{-1},$$

$$\alpha_{t2} = 0.5 \times 10^{-3} Kelvin^{-1},$$

$$\lambda_0 = 0.5 \times 10^9 Nm^{-2},$$

$$\lambda_1 = 0.5 \times 10^9 Nm^{-2},$$

$$j_0 = 0.185 \times 10^{-6} m^2,$$

$$\alpha_0 = .9 \times 10^3 N, \quad b_0 = .91 \times 10^3 N,$$

$$\tau_0 = .2, \quad \tau_1 = .4$$

$$\delta_1^2 = 1.3, \quad \delta_2^2 = 1.2,$$

$$\omega/\bar{\omega} = 10, \quad T_0 = 298 Kelvin.$$

The solid line and small dashes line represent magneto-thermo-microstretch elastic medium for LS-theory- MMT1 and for GL-theory- MMT2 respectively. The solid line and small dashes line with centre symbols represent thermo-microstretch elastic medium for LS-theory- MT1 and for GL-theory- MT2 respectively. Variations of amplitude ratios Z_i , with the angle of incidence θ_0 , for different waves are shown in Figs. 2–16.

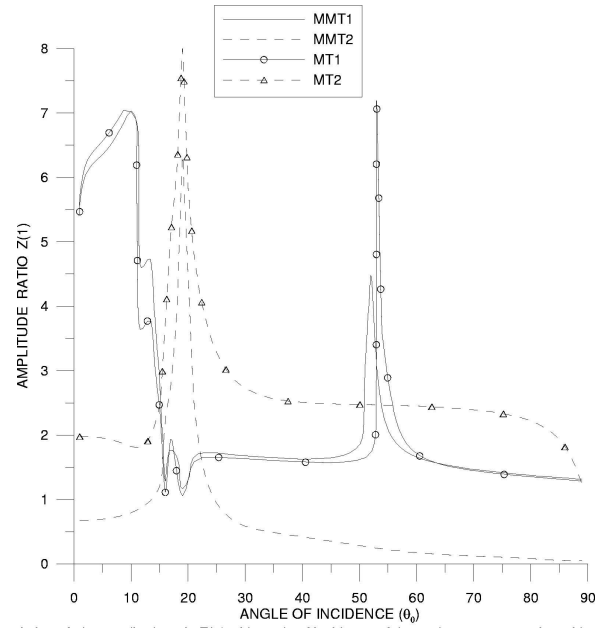


Fig. 2. Variation of the amplitude ratio $Z(1)$ with angle of incidence of thermal wave propagating with velocity V_2

T-wave. Figure 2 depicts that behavior of variations of amplitude ratio $Z(1)$ is similar for MMT1 and MT1 in the whole range. Also due to magnetic effect, the values of $Z(1)$ remain larger for MT2 in comparison to the values for MMT2, for all values of θ_0 (angle of incidence). It is noticed from Fig. 3

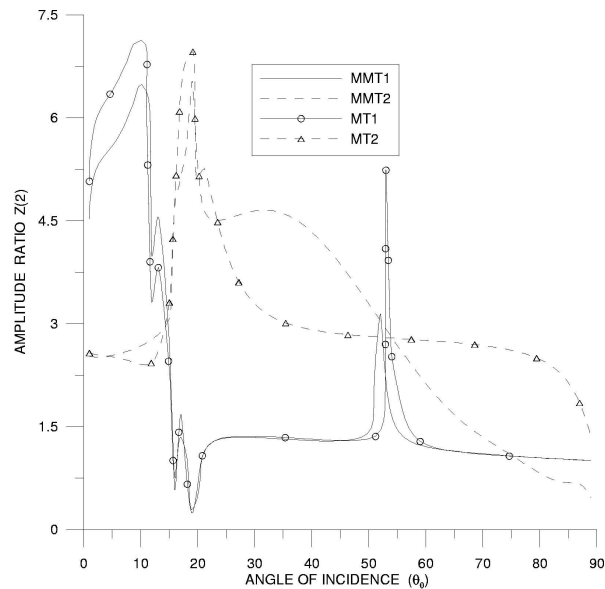


Fig. 3. Variation of the amplitude ratio $Z(2)$ with angle of incidence of thermal wave propagating with velocity V_2

that the behavior of variation of $Z(2)$ is similar for MMT1 and MT1 and oscillatory for MMT2 and MT2 respectively, in the whole range. The behavior of variations of $Z(3)$ (Fig. 4) is similar for MMT1 and MT1, in the whole range except when $50 \leq \theta_0 \leq 60$, where the values of $Z(3)$ are vary large

for MT1 in comparison to the values for MMT1. The values of $Z(3)$ are more for MT2 as compared to the values for MMT2 in the whole range except the difference between the values for MT2 and MMT2 is small in the range $10 < \theta_0 < 30$. The values of $Z(3)$ for MMT1 and MT1 have been shown in Fig. 4 by multiplying its original value by 10^{-1} respectively.

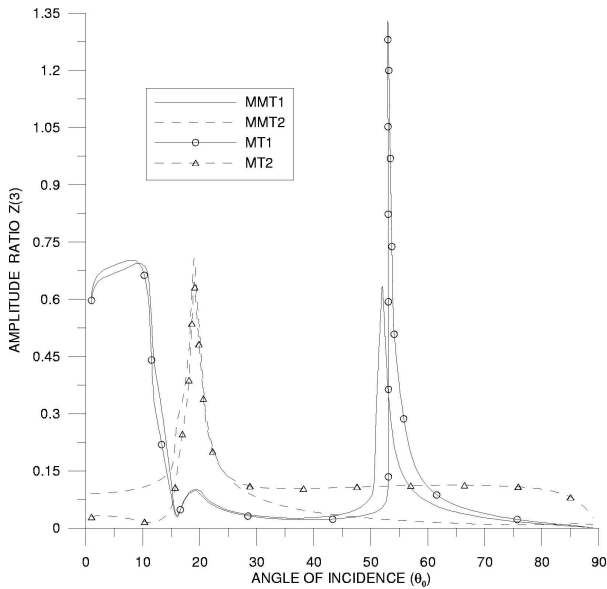


Fig. 4. Variation of the amplitude ratio $Z(3)$ with angle of incidence of thermal wave propagating with velocity V_2

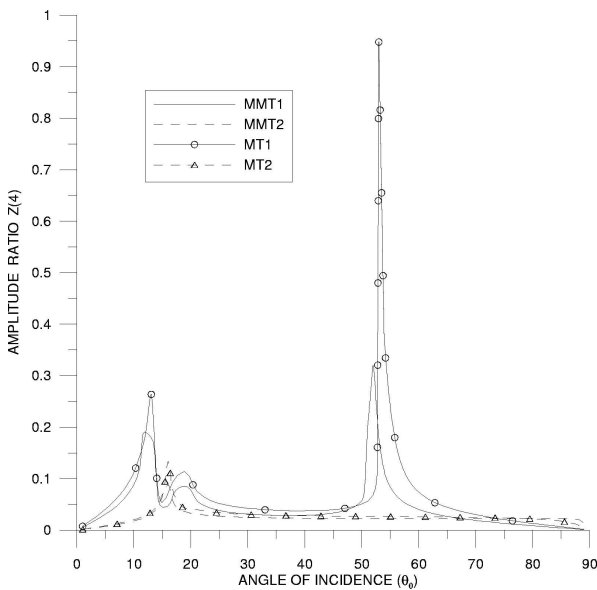


Fig. 5. Variation of the amplitude ratio $Z(4)$ with angle of incidence of thermal wave propagating with velocity V_2

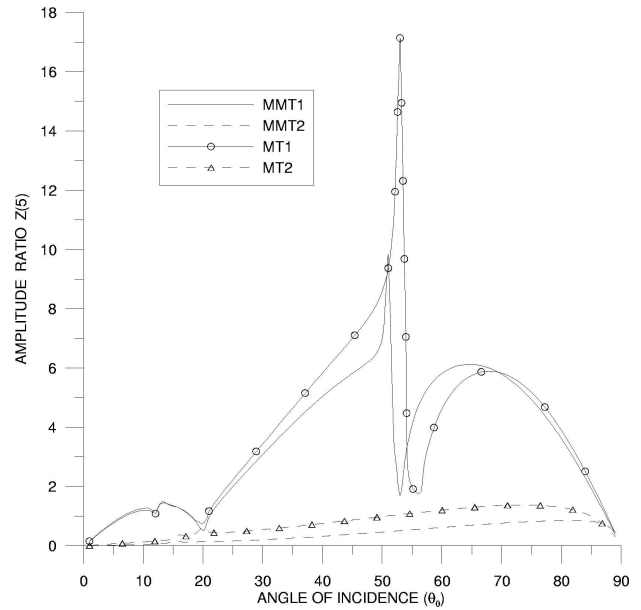


Fig. 6. Variation of the amplitude ratio $Z(5)$ with angle of incidence of thermal wave propagating with velocity V_2

Figures 5 and 6 depict that the behavior of variations of $Z(4)$ (Fig. 5) and $Z(5)$ (Fig. 6) is similar for MMT1, MT1 and also for MMT2, MT2 respectively, in the whole range, but the values of $Z(5)$ remain slightly more for MT2 in comparison to the values for MMT2, for all values of θ_0 .

LM-wave. Figure 7 depicts that due to magnetic effect, the values of $Z(1)$ are larger in the whole range for MT2 in comparison with the values for MMT2. Also the values for $Z(1)$ are smaller for LS theory (MMT1 and MT1) as compared to the values for GL theory (MMT2 and MT2), in the whole range. From Fig. 8 it is noticed that the trend of variations of

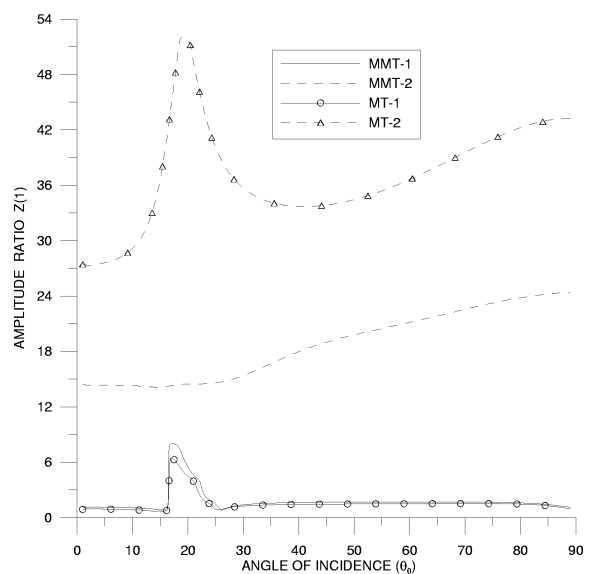


Fig. 7. Variation of the amplitude ratio $Z(1)$ angle of incidence of longitudinal microstretch wave propagating with velocity V_3

the values of $Z(2)$ for GL theory(MMT2 and MT2) is similar to the variations of $Z(1)$ (Fig. 7), in the range $0 \leq \theta_0 < 40$. The difference between the values of $Z(2)$ for MMT2 and MT2 decreases with further increase in angle of incidence. Also the behavior of variation of $Z(2)$ is similar for MMT1 and MT1, in the whole range. The values of $Z(2)$ for MMT2 and MT2 have been shown in Fig. 8 by multiplying its original value by 10^{-2} respectively. From Fig. 9 it is observed that the behavior of variations of $Z(3)$ is similar for MMT1 and MT1; MMT2 and MT2, but the values remain more for LS theory(MMT1 and MT1) as compared to GL theory(MMT2 and MT2), in the whole range.

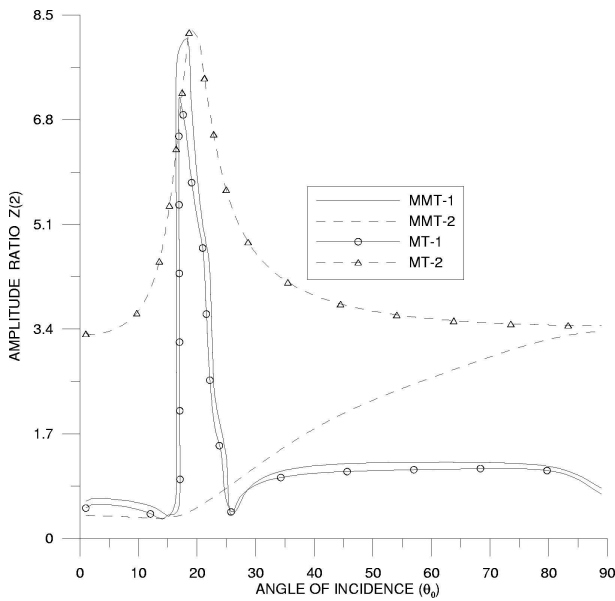


Fig. 8. Variation of the amplitude ratio $Z(2)$ angle of incidence of longitudinal microstretch wave propagating with velocity V_3

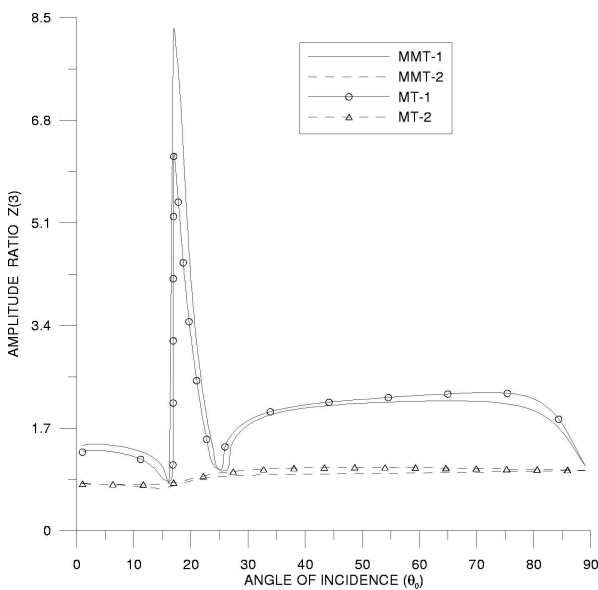


Fig. 9. Variation of the amplitude ratio $Z(3)$ angle of incidence of longitudinal microstretch wave propagating with velocity V_3

Figure 10 depicts that the values of $Z(4)$ are more for MT1 and MT2 as compared with the values for MMT1 and MMT2, in the whole range. The values of $Z(4)$ for MT2 have been shown in Fig. 10 by multiplying its original value by 10^{-1} . Figure 11 depicts the values of $Z(5)$ remain larger for MMT2 in comparison to the values for MT2, in the whole range, but for MMT1 and MT1 the behavior of variation is similar in the range $0 \leq \theta_0 \leq 20$ and as angle θ_0 increases, the values of MT1 become larger as compared with the values for MMT1.

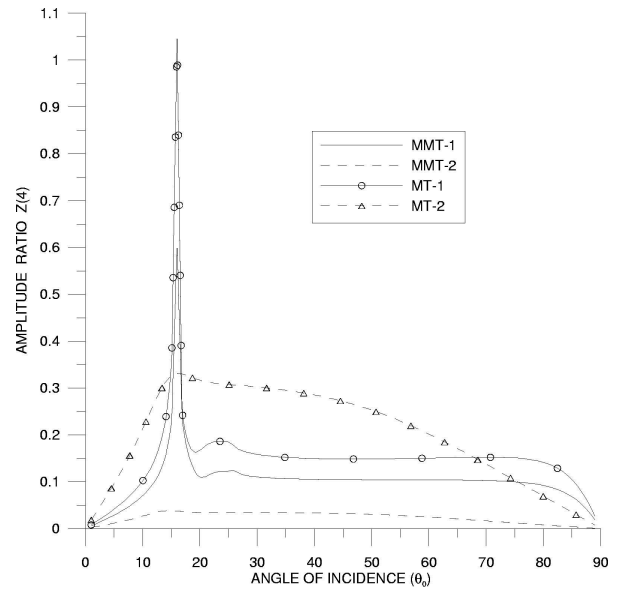


Fig. 10. Variation of the amplitude ratio $Z(4)$ angle of incidence of longitudinal microstretch wave propagating with velocity V_3

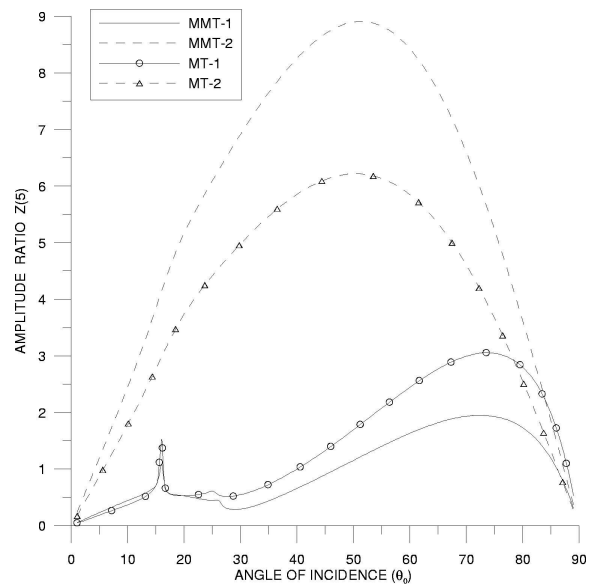


Fig. 11. Variation of the amplitude ratio $Z(5)$ angle of incidence of longitudinal microstretch wave propagating with velocity V_3

(CD-I)-wave. From Figs. 12–14 it is noticed that the behavior of variations of $Z(1)$, $Z(2)$ and $Z(3)$ respectively, is similar for MMT1 and MT1; MMT2 and MT2, with difference in the magnitude, in the whole range, but the values of $Z(1)$ for MT2, are slightly more in comparison to the values for MMT2 when $5 < \theta_0 < 25$, the values of $Z(3)$ for MT2 are more in comparison to the values for MMT2 in the range $5 < \theta_0 < 50$ and the values of $Z(2)$ (in Fig. 13) are more for MMT2 in comparison to the values for MT2 when $5 < \theta_0 < 35$. The values of $Z(3)$ for MT2 have been shown in Fig. 14 by multiplying its original value by 10.

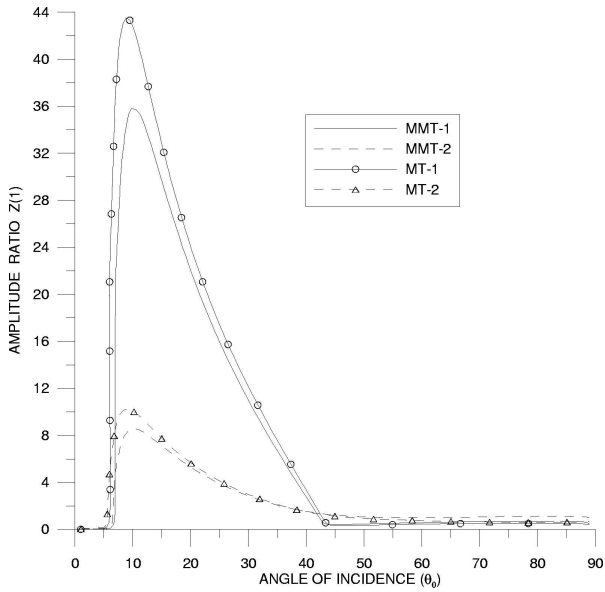


Fig. 12. Variation of the amplitude ratio $Z(1)$ angle of incidence of coupled transverse and microrotational (CD-I) wave propagating with velocity V_4

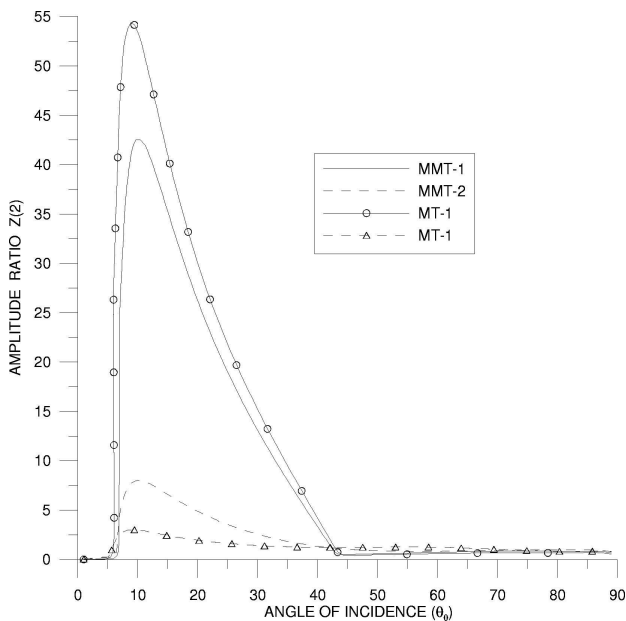


Fig. 13. Variation of the amplitude ratio $Z(2)$ angle of incidence of coupled transverse and microrotational (CD-I) wave propagating with velocity V_4

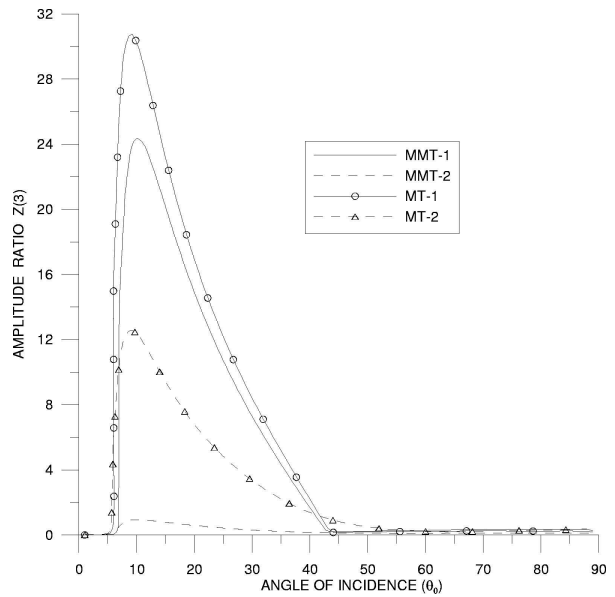


Fig. 14. Variation of the amplitude ratio $Z(3)$ angle of incidence of coupled transverse and microrotational (CD-I) wave propagating with velocity V_4

Figure 15 depicts that the values of $Z(5)$ are lowered to minimum for MT1 as compared with the values for MMT1, in the range $5 \leq \theta_0 < 40$, as the angle of incidence θ_0 increases the behavior of variations of $Z(4)$ is similar for all cases. From Fig. 16 it is noticed that the values of $Z(5)$ start with maximum for MMT1, but the trend of the variation for all cases is similar in the whole range.

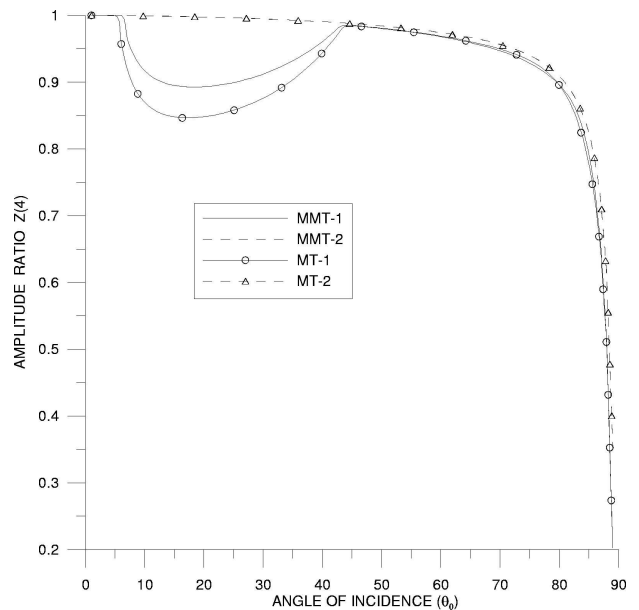


Fig. 15. Variation of the amplitude ratio $Z(4)$ angle of incidence of coupled transverse and microrotational (CD-I) wave propagating with velocity V_4

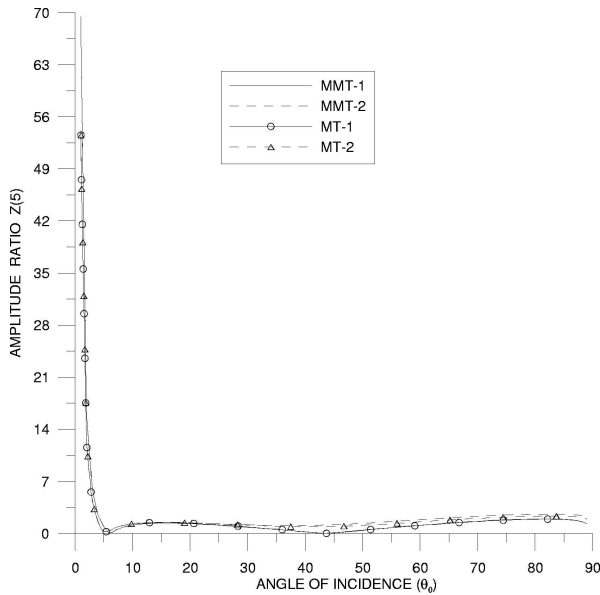


Fig. 16. Variation of the amplitude ratio $Z(5)$ angle of incidence of coupled transverse and microrotational (CD-I) wave propagating with velocity V_4

6. Conclusions

Detailed numerical calculations have been presented for the cases of thermal(T) wave, longitudinal microstretch(LM) wave and coupled transverse(CD-I) wave incident at the free surface of the model considered. Appreciable magnetic and thermal effects have been observed on the amplitude ratios, for the two theories of generalized thermoelasticity (L-S and G-L). The problem though theoretical, is of physical interest in the field of seismology, geophysics and earthquake engineering etc.

Acknowledgement. One of the authors Mr.Rupender is thankful to University Grants Commission for the financial support.

REFERENCES

- [1] H. Lord and Y. Shulman, "A generalized dynamical theory of thermo-elasticity", *J. Mech. Phys. Solid* 15, 299–309 (1967).
- [2] A.E. Green and K.A. Lindsay, "Thermoelasticity", *J. Elasticity* 2, 1–7 (1972).
- [3] M. Biot, "Thermoelasticity and irreversible thermodynamics", *J. Appl. Phys.* 27, 240–253 (1956).
- [4] I.M. Muller, "The coldness, a universal function in thermoelastic bodies", *Arch. Ration. Mech. Anal.* 41, 319–332 (1971).
- [5] A.E. Green and N. Laws, "On the entropy production inequality", *Arch. Ration. Mech. Anal.* 45, 47–53 (1972).
- [6] E.S. Suhubi, "Thermoelastic solids", in: ed. A.C. Eringen, *Continuum Physics*, Academic Press, London, 1975.
- [7] A.C. Eringen, "Micropolar elastic solids with stretch", *Ari. Kitabevi Matbassi* 24, 1–18 (1971).
- [8] A.C. Eringen, "Theory of thermo-microstretch elastic solids", *Int. J. Eng. Sci.* 28, 1291–1301 (1990).
- [9] A.C. Eringen, "Theory of thermo-microstretch fluids and bubbly liquids", *Int. J. Eng. Sci.* 28, 133–143 (1990).
- [10] A.C. Eringen, "Foundations of micropolar thermoelasticity", *Int. Cent. Mech. Studies, Course and Lectures* 23, 1970.
- [11] M. Nowacki, *Couple-stresses in the Theory of Thermoelasticity*, pp. 259–278, Springer-Verlag, Vienna, 1986.
- [12] S. Kaliski and W. Nowacki, "Wave-type equations of thermo-magneto-microelasticity", *Bull. Pol. Ac.: Tech.* 18(4), 325–333 (1970).
- [13] W. Nowacki, "Two-dimensional problem of micropolar magnetoelasticity", *Bull. Pol. Ac.: Tech.* 19(4), 307–311 (1971).
- [14] D.S. Chandrasekharaiah, "Heat flux dependent micropolar thermoelasticity", *Int. J. Eng. Sci.* 24, 1389–1395 (1986).
- [15] R. Kumar and B. Singh, "Wave propagation in a micropolar generalized thermoelastic body with stretch", *Proc. Ind. Acad. Sci.(Math.Sci.)* 106, 183–199 (1996).
- [16] R. Kumar and B. Singh, "Wave propagation of in generalized thermo-microstretch elastic solid", *Int. J. Eng. Sci.* 36, 891–912 (1998).
- [17] R. Kumar and B. Singh, "Reflection of plane waves from the flat boundary of a micropolar generalized thermoelastic half space with stretch", *Ind. J. Pure and App. Math.* 29, 657–669 (1998).
- [18] S.K. Tomar and M. Garg, "Reflection and transmission of waves from a plane interface between two microstretch solid half-spaces", *Int. J. Eng. Sci.* 43, 139–169 (2005).
- [19] R. Kumar and G. Pratap, "Reflection of plane waves in a heat flux dependent microstretch thermoelastic solid half space", *Int. J. App. Mech. and Eng.* 10(2), 253–266 (2005).
- [20] R. Kumar, D.S. Pathania, and J.N. Sharma, "Propagation of Rayleigh-Lamb waves in thermo-microstretch elastic plates", *Int. J. App. Mech. and Eng.* 12(4), 1147–1163 (2007).
- [21] B. Singh and R. Kumar, "Reflection of plane waves from the flat boundary of a micropolar generalized thermoelastic half-space", *Int. J. Eng. Sci.* 36, 865–890 (1998).
- [22] R.D. Gauthier, *Mechanics of Micropolar Media*, World Scientific, Singapore, 1982.